ResearchGate

See discussions, stats, and author profiles for this publication at: https://www.researchgate.net/publication/231632746

A High-Pressure Spectral Hole Burning Study of Correlation between Energy Disorder and Excitonic Couplings in the LH 2 Complex from Rhodopseudomonas Acidophila

ARTICLE *in* THE JOURNAL OF PHYSICAL CHEMISTRY B · JUNE 2002

Impact Factor: 3.3 · DOI: 10.1021/jp020540d

CITATIONS
20

READS
25

3 AUTHORS, INCLUDING:

Valter Zazubovich
Concordia University Montreal
43 PUBLICATIONS **714** CITATIONS
SEE PROFILE

Ryszard Jankowiak
Kansas State University
194 PUBLICATIONS **4,765** CITATIONS
SEE PROFILE

Available from: Ryszard Jankowiak
Retrieved on: 26 January 2016

A High-Pressure Spectral Hole Burning Study of Correlation between Energy Disorder and Excitonic Couplings in the LH 2 Complex from *Rhodopseudomonas Acidophila*

V. Zazubovich,* R. Jankowiak, and G. J. Small

Ames Laboratory, U.S. Department of Energy and Department of Chemistry, Iowa State University, Ames, Iowa 50011

Received: February 27, 2002

Low-temperature (5 K) nonphotochemical hole burning and absorption spectroscopies were used to study the effects of high pressure (up to 1015 MPa) on excitonic coupling energies and energy disorder in the light-harvesting complex 2 (LH 2) from *Rhodopseudomonas Acidophila* (strain 10050). The pressure dependences of the widths and positions of the B850 and B870 (lowest exciton level of the B850 ring) bands were determined. The results show, for the first time, that these parameters are linearly correlated (common scaling law), consistent with recent theoretical predictions (Jang; et al. *J. Phys. Chem. B* **2001**, *105*, 6655). Excitonic calculations for the B850 ring of bacteriochlorophyll *a* molecules were performed in the nearest dimer−dimer coupling approximation (Wu; et al. *J. Phys. Chem. B* **1997**, *101*, 7654) with E_{1+} diagonal energy disorder. Such a symmetry is known to dictate the response of the B870 level (absorption bandwidth, displacement (ΔE) from the B850 band maximum) to either diagonal or off-diagonal energy disorder. The results reveal that the pressure dependences of nearest neighbor coupling energies and the width of the distribution function for energy disorder are positively correlated, both increasing with pressure. Importantly, an effective pressure dependent excitonic Hamiltonian for the B850 ring was obtained. This Hamiltonian was used to show that mixing of the upper excitonic levels of the B850 ring in close proximity to the B800 levels is too weak to account for the additional (other than B800 → B850 energy transfer) decay channel of the B800 band. A simple combinatorial model for intra-B800 band downward energy transfer is presented that qualitatively explains all available low-temperature data on the additional decay channel.

1. Introduction

Pressure combined with absorption and spectral hole burning spectroscopies at low temperatures has been shown to be a very useful methodology for probing intermolecular interactions, excitonic structure, and excitation energy transfer (EET) dynamics associated with the Q_y (S_1) states of chlorophyll (Chl) molecules in photosynthetic antenna and reaction center complexes. Systems that have been studied include the light harvesting complex II (LHC II) of photosystem II of green plants,[1] the reaction center of photosystem II,[2] LH1[3,4] and LH2[5−8] complexes of purple bacteria, photosystem I of cyanobacteria,[9,10] and the chlorosome[11] and Fenna−Matthews−Olson antenna of the green sulfur bacterium *Chlorobium tepidum*.[12]

Concerning Chl−Chl coupling energies, it is the linear pressure shift (to the red) rate (R_p) of Q_y-absorption bands and zero-phonon holes (ZPH) burned into them that is the most informative, although pressure-induced broadening rates of absorption bands and ZPH can sometimes provide additional insights. At liquid helium temperatures, R_p values between ~ -0.05 and -0.15 cm^{-1}/MPa are expected for a Q_y state that is mainly localized on a single Chl (weak excitonic coupling). Values of $|R_p| \gtrsim 0.25$ cm^{-1}/MPa signal strong excitonic coupling to which electron-exchange interactions, in addition to Coulombic interactions, contribute. The former endows Q_y states with charge-transfer character that, unless the symmetry of the complex dictates otherwise, leads to a large permanent dipole moment change ($f\cdot\Delta\mu$) for the $S_0 \rightarrow Q_y$ transition, where f is the local field correction factor. (Stark hole-burning spectroscopy has proven to be a valuable technique for determining $f\cdot\Delta\mu$ values.[13]) By "large" is meant $f\cdot\Delta\mu > 1$ D. For photosynthetic complexes the value of f is often taken to be close to 1.5. Importantly, it has been found that there is strong positive correlation between R_p, $f\cdot\Delta\mu$, and the electron−phonon (protein) coupling strength, as recently discussed in refs 9 and 10. Both spectral hole burning and fluorescence line narrowing spectroscopies are now routinely used to characterize electron−phonon coupling, i.e., to determine mode frequencies, spectral profiles, and Huang−Rhys factors. Addition of pressure and external electric fields enhances the ability of spectral hole burning to resolve closely spaced absorption bands of different Q_y states. The red antenna states of Photosystem I serve as good examples of this.[9,10]

In this paper we present new high-pressure data on the cyclic LH2 (B800−850) bacteriochlorophyll *a* (BChl *a*) complex of *Rhodopseudomonas acidophila* (strain 10050) that provide new insights on the excitonic level structure of the B850 ring of strongly coupled BChl *a* molecules and the EET dynamics of the B800 ring of weakly coupled BChl *a* molecules. Although the excitonic structure and EET dynamics of the LH2 complex of purple bacteria have long been subjects of much interest (for reviews see refs 14 and 15), the determination of high-resolution X-ray structures of LH2 from *Rps. acidophila* (strain 10050)[16] and *Rhodospirillum molischianum*[17] stimulated even greater activity. As a result, femtosecond and hole burning experiments together with electronic structure calculations, which take into account the effects of energy disorder, have significantly

* Corresponding author: valterz@iastate.edu.

10.1021/jp020540d CCC: $22.00 © 2002 American Chemical Society
Published on Web 06/04/2002

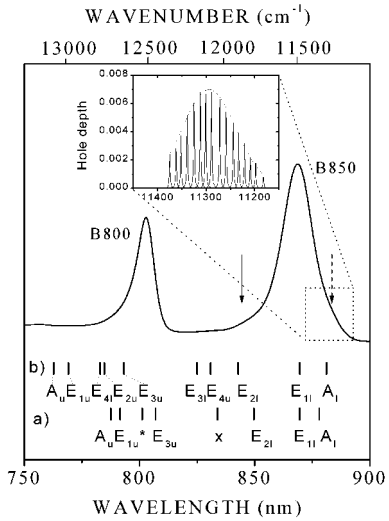

Figure 1. Absorption spectrum of LH 2 at 5 K and ambient pressure and B850 exciton level structures in the absence of disorder for (a) $V_l = -200$ cm^{-1}, $V_u = 110$ cm^{-1}, $V_{ul} = 135$ cm^{-1}, and $E_u - E_l = 580$ cm^{-1} and (b) $V_l = -260$ cm^{-1}, $V_u = 170$ cm^{-1}, $V_{ul} = 195$ cm^{-1}, and $E_u - E_l = 720$ cm^{-1}. E-levels are doubly degenerate. The asterisk denotes closely spaced E_{2u} and E_{4l} levels. The "×" denotes closely spaced E_{4u} and E_{3l} levels. Both level structures are positioned so that the E_{1l} level coincides with the B850 maximum. The solid and dashed arrows indicate absorption due to the E_{2l} and A_l levels, respectively. Inset: ZPH action spectrum of the B870 band and its Gaussian fit. The ZPHs shown are Lorentzian fits to observable holes.

improved our understanding of the light-driven processes of LH2, as reviewed in.[18]

The LH2 absorption spectra of *Rps. acidophila*, *Rs. molischianum*, and *Rhodobacter sphaeroides* exhibit two main BChl *a* absorption bands, B800 and B850, with maxima at ∼800 and 850 nm at room temperature. The structure of LH2 from *Rps. acidophila* revealed that it carries C_9 symmetry with the B800 ring being a 9-mer of BChl *a* monomers and the B850 ring a 9-mer of dimers whose two monomers are symmetry inequivalent with a Mg···Mg distance of 9.6 Å. The dimer is bound to the α,*β* polypeptide pair that binds a single B800 molecule. The distance between the nearest monomers of adjacent dimers is 8.9 Å. The resulting nearest neighbor BChl *a*−BChl *a* coupling energies are large, ∼300 cm^{-1}.[19] In contrast, the distance between adjacent B800 molecules is 21 Å, which results in weak coupling, ∼−25 cm^{-1}. It is generally held that the B800 Q_y states are highly localized on single B800 molecules, as reviewed in ref 18, The excitonic structure of the B850 ring, which is of particular importance to this paper, has been calculated by several groups.[19−24] (See also refs 25 and 26 for additional information on couplings for *Rps. Acidophila* and refs 27 and 28 for the excitonic structure of *Rs. Molischianum*.) Shown in Figure 1 are two B850 level structures calculated in the nearest dimer−dimer coupling approximation; see section 4. The exciton levels are labeled according to their C_9 symmetries with u and l denoting levels that originate from the upper and lower states of the basic dimer of the α,*β* polypeptide pair. The degenerate E_2, E_3, and E_4 levels are symmetry forbidden in absorption. The arrangement of the Q_y transition dipoles in the structure is such as to endow the E_{1l} level with almost all of the absorption intensity,[19,20] which is why it is placed at the B850 band maximum in Figure 1. Note that upper (u) B850 levels lie in the near vicinity of the B800 absorption band and that the A_l and E_{2l} levels are located on the low- and high-energy sides of the B850 band (the absorption spectrum was taken at 4.2 K; see ref 7 for its temperature dependence.)

As reviewed in ref 18, energy disorder (diagonal and/or off-diagonal), which stems from the intrinsic structural heterogeneity of proteins, destroys the cyclic symmetry. (Here we are interested in static disorder at low temperatures, rather than dynamic disorder that becomes important at high temperatures.) As a result, level degeneracies are removed, the zero-order levels mix, and the exciton states are no longer perfectly delocalized (extended). The extent of disorder-induced localization continues to be the subject of much discussion.[29,30] The reader interested in localization-extendedness patterns for diagonal and off-diagonal energy disorder is referred to ref 31. In the present paper the problem of energy disorder will be analyzed using the symmetry-based approach of Wu et al.,[21,31,32] rather than Monte Carlo type simulations. They introduced symmetry-adapted basis defect patterns (BDPs) that transform like the irreducible representations of the C_9 group and form a complete orthonormal set. That is, any arbitrary energy defect pattern, whether it is due to diagonal or off-diagonal disorder, can be written as a linear combination of the BDPs. The BDPs are most useful in the case of weak disorder where the disorder-induced couplings of the zero-order exciton levels are less than or similar to the zero-order level splittings, which is the case for the B850 ring. As an example of the usefulness of BDPs, we note that the forbidden A_l and E_{2l} exciton levels mix with the strongly allowed E_{1l} level (Figure 1) via a BDP of E_1 symmetry and, thereby, steal intensity from the E_{1l} level. The weak absorptions indicated by the solid and dashed arrows in Figure 1 were assigned to the E_{2l} and A_l levels, respectively.[32] The latter level is often referred to as B870. (The inset of Figure 1 is the ZPH action spectrum of the B870 at ambient pressure, which is discussed in section 3.) The weakness of the above two absorptions is consistent with weak disorder. It was found that consideration of only BDP of E_1 symmetry (there are two degenerate partners, E_{1+} and E_{1-}) provides a good description of the B850 band.[21] It was further shown that, for weak disorder, the effects of diagonal and off-diagonal disorder on the B850 band are similar.[31,32] Therefore, in this paper only diagonal disorder will be taken into account in the interpretation of high-pressure data for the B850 band. Concerning the B870 (A_l) band, Wu et al.,[33] using ZPH action spectroscopy, determined that for high-quality LH2 samples of *Rps. acidophila*, it lies 200 cm^{-1} below the B850 band maximum at 4.2 K and ambient pressure. This gap, together with the observation that the B870 band carries ∼3% of the absorption intensity of the entire B850 band and the ∼120 cm^{-1} inhomogeneous width of the B870 band were used to determine an effective Hamiltonian for the B850 ring.[21,31,32] Also taken into account was that a structural change that occurs at ∼150 K results in a ∼35% increase in the nearest neighbor BChl *a*−BChl *a* coupling energies.[7,21]

Also of relevance to this paper is the work of Silbey and co-workers.[24,34] Starting with the framework of Wu et al.,[21] they used degenerate perturbation theory to obtain analytic expressions for several spectroscopic properties of the B850 ring of the LH2 complex from *Rps. acidophila*, including the widths, positions, and absorption intensities of the B870 and split (by energy disorder) E_{1l} levels. Both diagonal and off-diagonal energy disorder were considered, as well as combinations of the two (uncorrelated, positively, and negatively correlated). Monte Carlo simulations showed that the analytic expressions are accurate for the weak disorder limit which, as already mentioned, applies to the B850 ring. A key finding was that the linear interdependencies exist between the above properties, as will be discussed in section 5. They also analyzed the single LH2 complex results (1.2 K) of Ketelaars et al.[35,36] who had

concluded that they are best explained in terms of elliptical distortion of the B850 ring. Silbey and co-workers were able to explain the results of Ketelaars et al. without recourse to elliptical distortion, although they did not suggest that such distortion does not occur. Their model also explained the results of Wu et al.[7,33] They also found, in agreement with the results of Wu et al.,[31,32] that for weak disorder the effects of diagonal and off-diagonal energy disorder are similar.

This brings us to the objective of the first part of this paper, which is to show, for the first time, how pressure dependent data can be used with theory to determine the linear pressure dependencies of BChl *a* site energies, excitonic couplings, and energy disorder, which are required for an understanding of how the excitonic level structure of the B850 ring of BChl *a* molecules varies with pressure. Importantly, the results are in accord with the prediction from the model of Silbey and co-workers (based on ambient pressure data) that linear interdependencies of key properties of the B850 band should exist.

The results of the first part of the paper are used in the second part that is concerned with the EET processes of the Q_y states associated with the B800 band. Of particular interest is the possible role of mixed B800−B850 states that involve the upper exciton levels of the B850 ring, Figure 1. Nonphotochemical hole burning studies of LH2 from *Rps. Acidophila*[5] and *Rb. Sphaeroides*[37] at liquid helium temperatures established that for excitation at the B800 band maximum and to lower energy, relaxation is dominated by B800 → B850 EET, which occurs in ∼2 ps. For both species the ZPH width was observed to increase in near linear fashion as the excitation was tuned to the blue of the band maximum. This additional decay channel for B800 was also detected at low temperatures in pump−probe experiments (see review by Sundström et al.[18]). For example, 783 nm excitation at the blue edge of the B800 band of *Rps. acidophila* (B800 absorption maximum at 803 nm) resulted in a lifetime of 400 fs.[5] Also, experiments on *single* complexes of *Rps. Acidophila*[38] at 1.2 K revealed that the widths of single B800 molecule absorption lines increased for frequencies to the blue of the B800 maximum. On the basis of Franck−Condon factor arguments it was concluded in ref 5 that the additional decay channel is unlikely to be due to excitation and subsequent relaxation of vibrations that build on the B850 origin band or the zero-point levels of B800 Q_y states. The high-energy tailing of the B800 band seen in Figure 1 was considered to be too intense to be due to vibronic transition. It was suggested that the tailing might be due to a mixed B800−B850 state(s). Some support for this came from circular dichroism experiments on LH2 of *Rb. Sphaeroides*.[39] Later, hole burning experiments of LH2 samples from *Rps. acidophila* which contain only one B800 molecule per complex firmly established that relaxation of excited vibrations plays no significant role in the additional decay channel.[40] This left only two plausible explanations: that it is due to downward intraband transfer involving only B800 molecules or to relaxation of mixed B800−B850 states that lie predominantly to the blue of the B800 band maximum. de Caro et al.[37] favored the former while Wu et al.[5] favored the latter. Wu et al. suggested that the mixed B800−B850 states could undergo downward relaxation to lower energy B800 and/or B850 states, but presented no calculations in support of this.

We present the results of high-pressure hole burning experiments and excitonic calculations that were designed to test the mixed B800−B850 state hypothesis. The basic idea behind our experiments was that if the mixed state hypothesis is correct, one might expect that the onset frequency of the additional decay channel relative to the B800 band maximum should vary with pressure. Such a variation was not observed, up to a pressure of 1015 MPa. Although it is difficult to argue against the existence of mixed states, it appears that the mixing is too weak to affect the onset of the additional decay channel. Finally, we show that the experimental hole widths can be explained with a combinatorial model in which downward transfer is dominated by transfer between nearest neighbor B800 molecules.

2. Experimental Section

Liquid cultures of *Rps. acidophila* 10050 were grown anaerobically at 30 °C in Pfenning media. Cells were harvested by centrifugation. Photosynthetic membranes were isolated by rupturing the whole cells in a French press and then solubilized using LDAO. Purification of LH 2 complexes obtained in this way is described in detail in ref 40. The samples were dissolved in 20 mM Tris−HCl buffer (pH = 8) containing 0.1% LDAO detergent. To ensure formation of a good quality glass, this solution was mixed with glycerol at a ratio of 1:2. Such mixing was performed just before inserting the sample into the pressure cell and cooling it down. This prevented extraction of B800 molecules from the LH2 complex by glycerol.[40]

Gelatin capsules (Torpac, no. 5) containing the sample were positioned in a Unipress GOC102 pressure cell with sapphire optical windows (8 mm thickness and 10 mm diameter). The distance between the window plugs (optical path length) was 3 mm. The cell was connected to a U11 3-stage hydraulic compressor through a flexible beryllium−copper capillary (o.d./i.d. = 3 mm/0.3 mm). Helium gas was used as the pressure-transmitting medium. The cell was cooled in a Janis 11DT helium cryostat. The cooling procedure was as follows: first, the cell was pre-cooled to about 190 K, next the pressure (slightly exceeding desired) was applied and then the cell was further cooled to liquid helium temperatures. Applying pressure at temperatures higher than 190 K resulted in plastic behavior, probably due to partial denaturation of the protein (see section 5). Attempts to apply pressures higher than ∼400 MPa at lower temperatures were unsuccessful due to leaking of the cell. To change the pressure during the experiment, the sample was heated to 190 K. Temperature was measured and stabilized with a Lakeshore Cryotronic model 330 temperature controller. A calibrated manganin resistance gauge (model MPG10, Unipress) was placed in the third stage of the compressor to measure the gaseous helium pressure. A calibration curve was used to determine the pressure on the sample upon solidification of the helium.

A Coherent 899 Ti−Sapphire tunable CW laser (2 GHz) line width pumped by a 15 W Coherent Innova 200 Ar-ion laser was used for hole burning. Combining the mid-wave optics set with a long-wave output coupler extended the wavelength range to 960 nm, sufficient for measuring the ZPH action spectrum of the B870 band due to the lowest exciton level of the B850 ring at high pressure. A burn intensity of ∼60 mW/cm^2 and burn time of 60 s (burn fluence of 3.6 J/cm^2) were used to obtain B870 action spectra. Holes in the low- and high-energy sides of the B800 band were burned with fluences of 2.5 and 20 J/cm^2, respectively.

A Bruker HR 120 Fourier transform spectrometer operated at a resolution of 0.5 cm^{-1} was used to record pre-burn and post-burn absorption spectra. The hole-burned spectrum is the post-burn spectrum minus the pre-burn spectrum.

3. Experimental Results

Figure 2 shows the absorption spectra of the LH2 complex from *Rps. Acidophila* at 0.1, 550, and 1015 MPa. The ambient

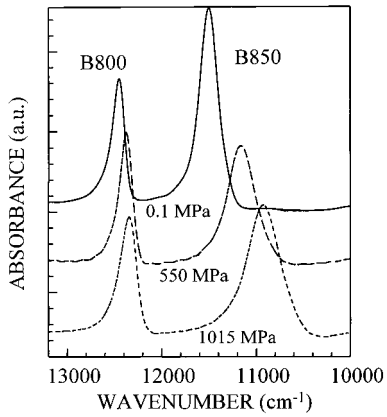

Figure 2. Absorption spectra of LH 2 at 7 K at ambient pressure (solid line), 550 MPa (long-dashed line), and 1015 MPa (short-dashed line). The B800−B850 energy gaps are 960, 1220, and 1420 cm^{-1}.

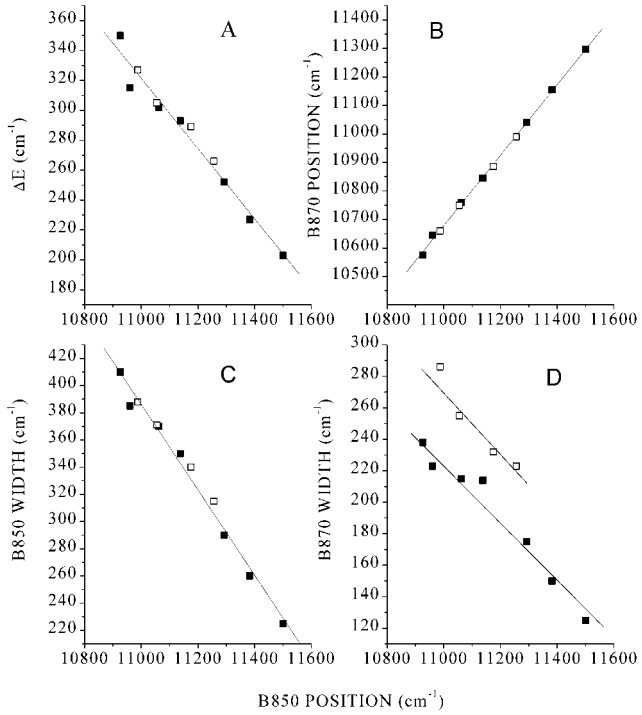

Figure 3. Dependences of (A) the gap between B850 and B870 band maximums, (B) B870 maximum position, (C) B850 bandwidth, and (D) B870 bandwidth on the position of the maximum of B850 band. (ΔE = −0.24 B850 position + 2906; B870 position = 1.24 B850 position − 2914; B870 width = −0.19 B850 position + 2313; B850 width = −0.31 B850 position + 3842. Also, B870 width = 0.80ΔE − 30. All numbers in cm^{-1}.) Solid squares correspond to $T_p \leq 190$ K and open squares correspond to $T_p = 230$ K, see text. The pressure was varied between 0.1 and 1015 MPa.

pressure spectrum, with B800 and B850 bandwidths (fwhm) of 145 and 210 cm^{-1}, is very similar to those obtained in our earlier studies.[5,33] As previously reported,[7] the pressure-induced shifting and broadening of the B850 band are considerably larger than those of the B800 band due to the strong excitonic coupling of the B850 ring. In Figure 3 the widths of the B850 and B870 (A_1 level) bands, the position of the B870 band and the energy gap (ΔE) between the B850 and B870 bands are plotted vs the B850 band position. Data were obtained at 5 K for eleven pressures ranging from ambient to 1015 MPa. (The rightmost data point is for ambient pressure in all frames A−D.) The B870 position and width were determined at each pressure using ZPH action spectroscopy where ZPH are burned at different wavelengths under constant burn fluence conditions.[41] The B870 ZPH action spectrum obtained at ambient pressure is shown in the inset of Figure 1. The width of the action spectrum is the inhomogeneous broadening of the B870 band. The linear correlations between the above four parameters and the B850 position are striking ($R \geq 0.98$). The solid data points were obtained by pressurizing at $T_p = 190$ K. At this and lower temperatures (results not shown) the pressure effects were elastic, as judged by the requirement that the absorption spectrum after pressure release was identical to the spectrum obtained at ambient pressure prior to pressurization ($T = 5$ K). Elasticity was not observed for $T_p = 230$ K, which temperature led to the open data points in Figure 3. (As discussed later, pressurization at 230 K leads to partial denaturation of the complex.) Nevertheless, the solid and open data points in frames A−C fall on the same straight line. Thus, the associated correlations with the B850 positions are not sensitive to sample "quality". However, this is not the case for the width of the B870 band, frame D. Explanations for these observations are given in section 5, where it is shown that the data in Figure 3 result from the pressure dependences of energy disorder and excitonic coupling being correlated.

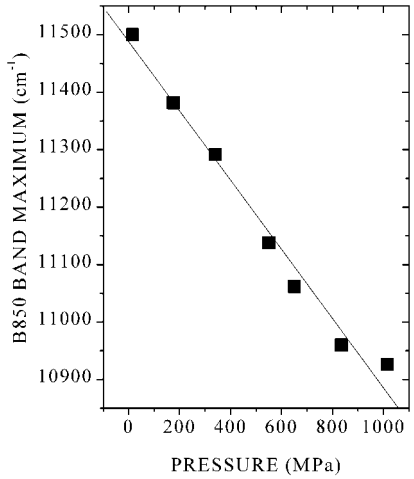

Figure 4. Pressure dependence of the B850 band maximum for T_p = 190 K. The shift rate is −0.57 cm^{-1}/MPa.

TABLE 1: Pressure-Induced Shifts and Broadening of LH-2 Bands

parameter	this work (T_p = 190 K)	previous work[7] (T_p = 80 K)	ratio
B800 shift (cm^{-1}/MPa)	−0.115[a]	−0.09	1.3
B850 shift (cm^{-1}/MPa)	−0.57	−0.40	1.4
B870 shift (cm^{-1}/MPa)	−0.72	−0.52	1.4
B800 broadening (cm^{-1}/MPa)	0.07	∼0[b]	N/A
B850 broadening (cm^{-1}/MPa)	0.19	0.13	1.4
B870 broadening (cm^{-1}/MPa)	0.12	0.09[c]	1.3
$d(\Delta E)/dp$ (cm^{-1}/MPa)	0.15	N/A	N/A

[a] Band shift rate; shift rates for the ZPHs are slightly larger. [b] See text for discussion. [c] Estimated from wavelength-dependent ZPH pressure shifts from ref 7.

Figure 4 shows the dependence of the B850 band peak position at 5 K on pressure for $T_p = 190$ K. The shift rate is −0.57 cm^{-1}/MPa. The shifts and broadening rates of the B800, B850, and B870 bands are given in Table 1 for $T_p = 190$ K. Note that values from this study are a factor of 1.3−1.4 larger than those reported in ref 7. In that work, however, maximum pressures of ∼350 and 75 MPa were applied at $T_p = 80$ and 12 K, respectively (shift and broadening rates were measured at 5 K). The factor of 1.3−1.4 is most likely due to the temperature

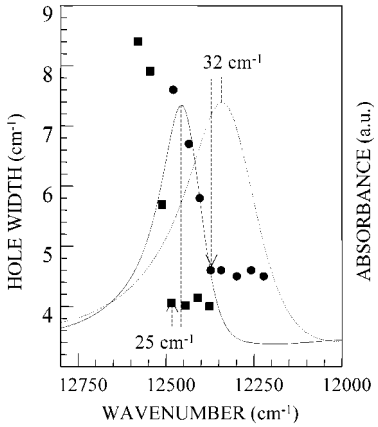

Figure 5. Absorption spectra and wavelength dependences of the hole width for ambient pressure (solid curve, squares) and for 875 MPa (dotted curve, circles). Lower energy holes (width $\sim$4 cm^{-1}) were burned with 25 mW/cm^2 for 100 s (2.5 J/cm^2). Fluences of 20 J/cm^2 were required to burn observable holes at the high-energy side of the B800 band. The two numbers are the displacement between the absorption maximum and the onset of the hole broadening.

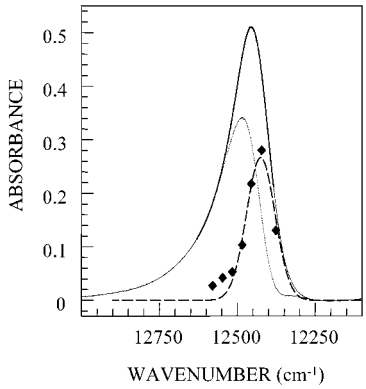

Figure 6. B800 absorption spectrum (solid line) and the burn energy dependence of the depth of spectral holes burned with a fixed fluence of 2.5 J/cm^2 at ambient pressure (diamonds). The dashed curve is the Gaussian fit to hole depth dependence, which is normalized to account for 30% of the B800 band's integrated absorption; see Discussion. The dotted profile is the difference between the absorption spectrum and the above Gaussian. It represents the absorption profile of Bchl *a* molecules capable of downward intraband energy transfer.

dependence of the isothermal compressibility κ. The pressure shift rate of the B850 band at $T_p = 160$ K is -0.5 cm^{-1}/MPa (data not shown) A value of -0.89 cm^{-1}/MPa at room temperature was reported in ref 8. That the broadening rate for the B850 band is larger than that of the B870 bands is reasonable since the B850 band consists of two components due to the splitting of the E_{1l} level by energy disorder. Increasing pressure leads to an increase of the splitting and broadening of the two components; see section 5. That broadening was not observed in ref 7 for the B800 band is most likely due to the maximum pressure used being only 350 MPa ($T_p = 80$ K). With the above $\sim$1.4 scaling factor and the $T_p = 190$ K broadening rate, the broadening rate for $T_p = 80$ K is 0.05 cm^{-1}/MPa, which for 350 MPa results in a broadening of only $\sim$17 cm^{-1} Given that the B800 bandwidth at ambient pressure is 145 cm^{-1}, it is not surprising that broadening was not detected.[7] We note that the B870 broadening rate of 0.09 cm^{-1}/MPa in Table 1 was estimated using wavelength-dependent ZPH pressure shift rates from ref 7.

As mentioned in the Introduction, the intensity of the B870 band relative to that of the entire B850 band is important for gauging the extent of energy disorder, as measured relative to the strength of excitonic coupling in the B850 ring. Following the procedure given in ref 33 (but improved by taking the contribution of E_{2l} levels into account), which relies on the ZPH action spectrum of B870, we determined that the integrated intensity of the B870 band at all pressures is 5.5 $\pm$ 1.5% of the total intensity of the B850, compared with the value of $\sim$3% reported in ref 33.

We present next the hole burning data that pertain to the additional B800 intraband relaxation channel. ZPHs were burned across the B800 band at 5 K at pressures of 0.1, 290, 610, 875, and 1015 MPa. Results at ambient pressure and 875 MPa are shown in Figure 5. They, as well as the data for the other pressures, showed that the onset of the increase of the ZPH width follows the shift of the B800 band maximum. For all pressures that onset position is 27 $\pm$ 5 cm^{-1} to the blue of the B800 absorption maximum. No significant influence of pressure on the hole width was observed for the low-energy side of the B800 band. (Widths of $\sim$4.0$-$4.5 cm^{-1} were measured for shallow holes ($\sim$0.05 fractional hole depth), which correspond to B800 $\rightarrow$ B850 energy transfer times of 2.4 $\pm$ 0.2 ps, in close agreement with values in ref 6). That pressure does not significantly affect the B800 $\rightarrow$ B850 energy transfer rate is also in agreement with the results reported in ref 6. Low-pressure ($p < 70$ MPa) tuning of spectral holes burned into the B800 band revealed a weak dependence of the pressure shift rates on burning wavelength. The average rate is -0.135 ± 0.010 cm^{-1}/MPa. Shift rates slightly smaller than average were observed near the B800 band maximum; shift rates slightly larger than average (up to -0.145 cm^{-1}/MPa) were observed for the lowest energy holes. The rates of the ZPH shifts are somewhat larger than the shift rate of the peak frequency of B800 band. The value of -0.145 cm^{-1}/MPa was used as the Bchl *a* monomer shift rate in the excitonic calculations for the B850 ring. It is important to point out that pressure shift rates for $^1\pi\pi^*$ states of isolated chromophores in polymers, glasses, and proteins[42$-$45] and Q_y states of photosynthetic complexes that are highly localized on a single Chl molecule[7,12] are ~-0.05 to -0.15 cm^{-1}/MPa. Thus, the shift rate for B800 is consistent with the excitations of the B800 ring being highly localized.

Figure 6 shows the wavelength dependence of the ZPH depth (5 K) at ambient pressure (diamonds). These holes were burned with 25 mW/cm^2 for 100 s. The fractional hole depth is only about 0.03. The resulting ZPH action spectrum represents the site energy distribution function (SDF) for sites whose decay is determined by B800 $\rightarrow$ B850 transfer. The Gaussian fit to the action spectrum, normalized to account for 30% of integral absorption of B800 band (see section 5B), provides a good fit to the low-energy edge of the B800 band. This is also the case for the 875 MPa action spectrum (results not shown). It is interesting to note that the ratio of widths of the action spectrum for the two pressures is equal to the ratio of B800 bandwidths and to the ratio of the shifts of action spectrum maximum from the B800 band maximum (Table 2).

4. Overview of Exciton Theory for the B850 Ring

For the exciton calculations the formalism of Wu et al.[21,32] was used. They employed the nearest dimer$-$dimer coupling approximation, where the dimer is that of the α,β polypeptide pair (as defined earlier) and used a delocalized (*k*-space) exciton basis set. There are several advantages to their symmetry-based approach, including that the absorption intensities of the 18 exciton levels in the presence of energy disorder are determined

TABLE 2: Properties of the B800 Band and Its Low-Fluence Hole Burning Action Spectrum

press. (MPa)	B800 band max. (cm^{-1})	action spectrum peak freq (cm^{-1})	dist between peaks (cm^{-1})	B800 width (cm^{-1})	action spectrum width (cm^{-1})
0.1	12 457	12 427	30	150	110
870	12 359	12 320	39	200	145
ratio			0.77	0.75	0.76

by the eigenvector components corresponding to the allowed E_{1l+} and E_{1l-} levels, where + and − indicate the two components of the E_{1l} level. In the absence of disorder, the Hamiltonian in the site representation is

$$H_0 = \sum_{i=u,l}[E_i\sum_{\alpha=0}^{n-1}|\alpha_i\rangle\langle\alpha_i| + V_i\sum_{\alpha,\beta=0}^{n-1}{}'|\alpha_i\rangle\langle\beta_i|] + V_{ul}\sum_{\alpha,\beta=0}^{n-1}{}'[|\alpha_l\rangle\langle\beta_u| + |\beta_u\rangle\langle\alpha_l|] \quad (1)$$

where α and β label the dimers ($n = 9$ for B850 ring of *Rps. Acidophila*). The index i = u and l denotes upper and lower levels of the basic dimer, with energies E_u and E_l. By transforming from the site representation to the delocalized (k space) representation, one obtains from the first square-bracketed term[21]

$$E_l^k = E_l + 2V_l\cos(2\pi k/n) \qquad k = 0, 1, n-1 \quad (2)$$

and

$$E_u^k = E_u + 2V_u\cos(2\pi k/n) \quad (3)$$

Similarily, one finds from the V_{ul} term in eq 1 that[21]

$$V_{int}^k = 2V_{ul}\cos(2\pi k/n) \quad (4)$$

which is the coupling energy between upper and lower delocalized exciton levels. Symmetry dictates that only levels of the same symmetry (k value) can couple. The correspondence between the k values and the irreducible representations of the C_9 group is as follows: $k = 0$ (A), $k = 1, 8$ (E_1), $k = 2, 7$ (E_2), $k = 3, 6$ (E_3), and $k = 4, 5$ (E_4); see Figure 1. The nearest neighbor dimer−dimer coupling energies can be obtained from the monomer−monomer coupling.[3] Let A_1B_1 and A_2B_2 be nearest neighbor Bchl *a* dimers, so that the dimer−dimer coupling potential is

$$V = V_{A_1A_2} + V_{B_1B_2} + V_{A_1B_2} + V_{B_1A_2} \quad (5)$$

V_l, V_u, and V_{ul} can be obtained from

$$\langle 2^{-1/2}(A_1^*B_1A_2B_2 \pm A_1B_1^*A_2B_2)|V|2^{-1/2}(A_1B_1A_2^*B_2 \pm A_1B_1A_2B_2^*)\rangle \quad (6)$$

where the functions in the bra and ket are the normalized excited-state wave functions for dimer 1 and 2, respectively. The ++, − −, and + − combinations correspond to V_u, V_l, and V_{ul}, respectively. Therefore,

$$V_l = \frac{1}{2}(\langle V_{A_1A_2}\rangle + \langle V_{B_1B_2}\rangle - \langle V_{A_1B_2}\rangle - \langle V_{B_1A_2}\rangle) \quad (7)$$

$$V_u = \frac{1}{2}(\langle V_{A_1A_2}\rangle + \langle V_{B_1B_2}\rangle + \langle V_{A_1B_2}\rangle + \langle V_{B_1A_2}\rangle) \quad (8)$$

$$V_{ul} = \frac{1}{2}(\langle V_{A_1A_2}\rangle - \langle V_{B_1B_2}\rangle - \langle V_{A_1B_2}\rangle + \langle V_{B_1A_2}\rangle) \quad (9)$$

where, for example,

$$\langle V_{A_1A_2}\rangle = \langle A_1^*A_2|V_{A_1A_2}|A_1A_2^*\rangle \quad (10)$$

Sauer et al.[19] calculated the values for the matrix elements in eqs 7−9 using the room-temperature X-ray structure of the LH 2 complex of *Rps. Acidophila*. They are −50, −36, 12, and 290 cm^{-1}, respectively. With these values eqs 7−9 lead to $V_u = 110$ cm^{-1}, $V_l = -200$ cm^{-1}, and $V_{ul} = 135$ cm^{-1}.

In the presence of energy disorder, the Hamiltonian is

$$H = H_0 + H_\lambda + H_\nu \quad (11)$$

where H_λ describes the diagonal and H_ν the off-diagonal disorder. Starting with the standard expressions for H_λ and H_ν in the site representation, Wu et al.[32] derived the expressions for coupling between delocalized states of a C_n ring due to either H_λ or H_ν. Since in this paper only diagonal energy disorder is considered, we give only the result for H_λ:

$$\langle k|H_\lambda|k'\rangle = \frac{1}{n}\sum_{\alpha=0}^{n-1}\lambda_\alpha B^{(k-k')\alpha} \quad (12)$$

where λ_α is the energy defect at site α and $B = \exp(i2\pi/n)$. Any arbitrary energy defect pattern can be calculated as a superposition of basic defect patterns (BDP) starting with an energy defect λ_0 at site "0". The selection rule for coupling delocalized exciton states k and k' is

$$k - k' = \pm j \quad (13)$$

where the active BDP is $E_{\pm j}$, with ± indicating the degenerate patterns of the E_j BDP. Equations 12 and 13 apply to mixing within the upper and lower manifolds as well as to mixing of upper and lower levels. Equation 13 also applies to off-diagonal disorder.

Wu et al.[21,32] showed that the energy and absorption intensity of the lowest energy B870 (A_l) level is determined by the E_1 BDPs. From Figure 1 and eq 13 one sees that they couple the E_{1l} level with both the A_l and E_{2l} levels. Since the B870 band is of primary interest, the results of calculations reported here were obtained with the E_{1+} BDP (the E_{1-} BDP gives identical results, vide infra). The BDP defect patterns are given in refs 21 and 32. One expects, of course, that on average all BDPs should carry equal weight for random disorder, it is just that the E_1 BDP is of primary importance for the B870 band. Such a finding would be very difficult to deduce from Monte Carlo simulations on the effects of energy disorder.

To understand the effects of pressure on the B850 exciton levels, one needs to know the pressure dependence of the distribution function that governs energy disorder. Following the procedure in ref 21, the dependences of the energy gap (ΔE) between the E_{1l} and B870 levels and the absorption intensity of the B870 band on the disorder parameter λ_0 for the E_{1+} BDP were determined. Structural fluctuations from complex to complex were taken into account by introducing a Gaussian distribution function for λ_0, with half-width $W(\lambda_0)$. As explained in ref 21, the shape of the B870 band is the product of the function that describes the dependence of the B870 band intensity on λ_0 and the half-Gaussian distribution function for λ_0. Thinking in terms of single complexes, the just mentioned product reflects the fact that as ΔE increases relative to its value

in the absence of disorder, the intensity of the B870 level must increase, but the probability of finding a complex with larger ΔE decreases.

Also required are the pressure dependencies of V_l, V_u, V_{ul}, $E_u - E_l$, and the Bchl *a* monomer excitation energy. As mentioned, the last was set to equal the shift rate of -0.145 cm^{-1}/MPa, determined for the ZPH burned into the B800 band. On the basis of the results in ref 21, it is clear that the coupling of upper and lower levels (eq 4) should have a small effect on the ΔE and the widths of the E_{1l} and B870 levels that contribute to the B850 band. Thus, we first ignored that coupling in order to obtain the first approximation for dV_l/dp by simulating the dependence of the B870 bandwidth on ΔE, frames A and D in Figure 3 ($T_p = 190$ K). In doing so it was necessary to account for the pressure dependencies of both V_l and $W(\lambda_0)$, as discussed in section 5. (The values obtained are, respectively, -0.21 and 0.15 cm^{-1}/MPa.) Next, the effects of coupling between the upper and lower levels were examined. This requires values for dV_u/dp and dV_{ul}/dp. They were set equal to negative of the dV_l/dp. The reasoning here stems from eqs 7−9, in which $\langle V_{B_1A_2} \rangle$ is by far the largest contributing term, one that is significantly contributed to by electron-exchange coupling between B_1 and A_2 molecules.[3] Thus, it was deemed reasonable to neglect the pressure dependence of the other three terms. Through an iterative procedure, refined values of dV_l/dp and $dW(\lambda_0)/dp$ were determined and an estimate for $d(E_u - E_l)/dp$ was obtained.

5. Discussion

A. Pressure Dependence of the B850 Ring Exciton Structure. In this subsection a theoretical interpretation of the results in Figure 3 for $T_p = 190$ K is provided. They show that ΔE, the B850 bandwidth, B870 band position, and width are strongly cross-correlated. As will be shown, this means that the pressure dependencies of exciton couplings and energy disorder are positively correlated. Based on the results in Table 1, these dependencies can be expected to depend also on T_p. Before proceeding, a few comments on the $T_p = 230$ K data points (open squares) in Figure 3 are in order. Pressurization (maximum pressure of 870 MPa) at that temperature led to plastic behavior and large B800 and B870 bandwidths at 5 K and ambient pressure, ~250 and ~180 cm^{-1}, respectively. The corresponding values for $T_p = 190$ K are 145 and 125 cm^{-1} (similar values were obtained in earlier studies with lower pressurization temperatures where elastic behavior was also observed[7,33]). The plastic behavior indicates that the LH2 complex underwent partial denaturation at 230 K and high pressure (see refs 46 and 47 and references therein). We note that the width of ~240 cm^{-1} for the B800 band at ambient pressure and 1.2 K obtained by Ketelaars et al.[36] based on single complex excitation spectra is similar to the 250 cm^{-1} width for $T_p = 230$ K. They did not comment on the large difference between their width and the widths obtained in bulk experiments with high-quality samples, ~120 cm^{-1}. As mentioned earlier, they interpreted their single complex results for the B850 ring in terms of elliptical distortion. It is conceivable that such distortion is, to a considerable extent, due to the spin-coating procedure used to imbed LH2 complexes in the thin polymer films that yielded excessive inhomogeneous broadening of the B800 band.

Excitonic Calculations with Neglect of Coupling between the Upper (u) and Lower (l) Exciton Levels of the B850 Ring. With this neglect, $V_{ul} = 0$ in the Hamiltonian defined by eq 1. For reasons given earlier only diagonal energy disorder due to the E_{1+} BDP was considered since BDPs of other symmetries, excluding E_{1-}, have little effect on the B870 band, specifically its width, displacement (ΔE) from the B850 band maximum, and intensity. We confirmed the result stated in refs 21, 31, and 32 that the effects of E_{j+} and E_{j-} BDPs are identical if $\lambda_{0,+}N_{j,+}^{-1} = \lambda_{0,-}N_{j,-}^{-1}$ where $N_{j,\pm}$ is the BDP normalization constant given by

$$N_{j,\pm} = \frac{1}{\sqrt{\sum_{\alpha=0}^{n-1}\left[\cos\left(\frac{2\pi j\alpha}{n}\right) \pm \cos\left(\frac{2\pi j(\alpha-1)}{n}\right)\right]^2}} \quad (14)$$

and λ_{0+} and λ_{0-} are the energy defects at site "0". Thus, the E_{1+} and E_{1-} BDP have the same effect on the B870 band for the same degree of energy disorder. We use that band to arrive at first approximations for the values of dV_l/dp and $dW(\lambda_0)/dp$; vide supra. The results presented below were obtained using eqs 2 and 12. We emphasize again that since the weak energy disorder limit applies, one can expect similar results for diagonal and off-diagonal energy disorder. A value of -320 cm^{-1} was used for V_l at ambient pressure in the low-temperature limit.[21] That value with E_{1+} disorder is consistent with the experimental findings in ref 33 that $\Delta E = 200$ cm^{-1} and the width of B870 SDF is 120 cm^{-1}. It was mentioned earlier that $V_l = -200$ cm^{-1} based on excitonic calculations by Sauer et al.[19] That value is too small to account for the ΔE and B870 bandwidth data in Figure 3; vide infra.

The interdependencies of ΔE, the B870 bandwidth and the B850 band position were first investigated for fixed $W(\lambda_0)$ and varying V_l and fixed V_l and varying $W(\lambda_0)$. Some results are given in Tables 3 and 4. Also listed are the B870 band intensity (relative to the intensity of the entire B850 band) and the positions of the B850 and B870 band maxima relative to $E_l = 0$ (eq 2). The positions of the band maxima are informative but of lesser importance since they depend on coupling between

TABLE 3: Properties of Lowest-Exciton Levels of B850 for Various V_l and Fixed Half-Widths of λ_0 Distribution of 140 cm^{-1} (Coupling between Upper and Lower B850 Levels Neglected)

V_l (cm^{-1})	B850 max. (cm^{-1})[a]	B870 max. (cm^{-1})[a]	ΔE (cm^{-1})	B870 width (cm^{-1})	integral intensity of B870[b]
−300	−460	−647	187	105	1.00
−320	−488	−686	198	102	0.93
−375	−575	−794	219	97	0.74
−450	−689	−945	256	90	0.55

[a] Numbers were obtained with $E_l = 0$ (see eq 2). [b] Integral intensity of 1 corresponds to about 10% of total B850 absorption being due to the B870 band.

TABLE 4: Properties of Lowest-Exciton Levels of B850 for Various Half-Widths of Distribution of λ_0 and Fixed V_l = 300 cm^{-1} (Coupling between Upper and Lower B850 Levels Neglected)[a]

$W(\lambda_0)$ (cm^{-1})	B850 max. (cm^{-1})	B870 max. (cm^{-1})	ΔE (cm^{-1})	B870 width (cm^{-1})	integral intensity of B870[b]
100	−460 ± 2	−632	172	68	0.77
120	−460 ± 2	−639	179	86	0.89
140	−460 ± 2	−647	187	105	1.00
160	−460 ± 2	−655	195	122	1.10
180	−460 ± 2	−662.5	202.5	141	1.18
200	−460 ± 2	−669.5	209.5	159	1.24

[a] Numbers in second and third columns were obtained by taking $E_l = 0$; see eq 2. [b] Integral intensity of 1 corresponds to about 10% of total B850 absorption being due to the B870 band. As in Table 3, this value corresponds to $V_l = -300$ cm^{-1} and $W(\lambda_0) = 140$ cm^{-1}.

the upper and lower dimer levels and on the coupling that determines the $E_u - E_l$ energy gap; vide infra. The results in Table 3 show that as V_l increases from -300 cm^{-1} with $W(\lambda_0)$ constant at 140 cm^{-1}, ΔE increases, as expected. However, the B870 band narrows, in disagreement with the data in frame D of Figure 3, which show that increasing pressure, which leads to increasing V_l (negative direction), also leads to increasing B870 bandwidth, as measured by ZPH action spectroscopy. The narrowing effect seen in Table 3 is presumably due to the motional narrowing from excitonic delocalization that increases as $V_l/W(\lambda_0)$ increases.[48] One also observes that the intensity of the B870 band decreases with increasing V_l. This is expected since with increasing $V_l/W(\lambda_0)$ the mixing of the zero-order exciton levels due to energy disorder decreases, which results in the B870 level borrowing less intensity from the allowed E_{1l} levels. Turning to Table 4 for $V_l = -300$ cm^{-1} and $W(\lambda_0)$ increasing from 100 cm^{-1}, one sees that the B870 band broadens with the increasing $W(\lambda_0)$ and that the intensity increases. Both trends are expected since increasing energy disorder for fixed V_l leads to increasing mixing between the E_{1l} and B870 levels and increasing inhomogeneous broadening (decreasing motional narrowing). For the range of disorder considered, the B850 band position is independent of the degree of disorder for fixed V_l (-300 cm^{-1}). This was found also for the other values of V_l considered. Analysis of the E_{1l+} and E_{1l-} exciton level positions and intensities revealed that their disorder-induced shifts are in opposite directions. Furthermore, the different magnitudes of the shift rates were compensated by different intensities of the two components in such a way that the maximum of the calculated B850 band was independent of the degree of disorder. In the calculations the homogeneous broadening of $\sim$50 cm^{-1} of the E_{1l+} and E_{1l-} levels due to $\sim$100 fs downward intereexciton level relaxation (see refs 18 and references therein) was taken into account. Because of the above independence, we defined ΔE as the gap between the B850 band maximum and the maximum of the B870 band.

From the results in Tables 3 and 4 and experimental findings that with increasing pressure both the B850 and B870 bands shift and broaden, ΔE increases, and the B870 band intensity does not change significantly (vide infra), it is clear that the pressure dependencies of both V_l and $W(\lambda_0)$ need to be taken into account. We emphasize that the monomer Bchl *a* pressure shift rate has no effect on ΔE and the width and intensity of the B870 band. Figure 7 shows the results of our analysis for the B870 bandwidth and ΔE. The solid squares are experimental data points ($T_p = 190$ K) from frames A and D of Figure 3. From left to right the data points correspond to pressures of 10, 175, 340, 550, 650, 835, and 1015 MPa. It is apparent that the bandwidth and ΔE are linearly correlated. The open squares with thin solid lines drawn through them show the calculated dependence of the bandwidth on ΔE for different fixed values of V_l (-300, -375, -450, -525 cm^{-1}) and variable $W(\lambda_0)$. The dashed lines show the calculated dependence of the bandwidth on ΔE for different fixed values of $W(\lambda_0)$ and variable V_l. The grid pattern formed by the thin solid and dashed lines allows for easy approximate determination of the V_l and $W(\lambda_0)$ values for any data point. For example, for the ambient pressure point ($\Delta E = 200$ cm^{-1} B870 width = 125 cm^{-1}) $V_l = -315$ cm^{-1} and $W(\lambda_0) = 160$ cm^{-1}, in good agreement with the values in ref 21. For the 1015 MPa data point ($\Delta E = 350$ cm^{-1} bandwidth = 237 cm^{-1}) $V_l \approx -525$ cm^{-1} and $W(\lambda_0) \approx 310$ cm^{-1}. These numbers (as well as those for other data points) lead to dV_l/dp of -0.21 cm^{-1}/MPa and $dW(\lambda_0)/dp = 0.15$ cm^{-1}/MPa. It is important to emphasize that Figure 7 establishes that the magnitudes of V_l and $W(\lambda_0)$ are positively correlated in their response to pressure. To the best of our knowledge this is the first determination of such correlation in a photosynthetic complex. Finally, we note that a grid pattern of the type shown in Figure 7 can be obtained for the B850 bandwidth vs ΔE, although with greater effort since the splitting of the degeneracy of the E_{1l} levels is determined by BDPs of different symmetries.

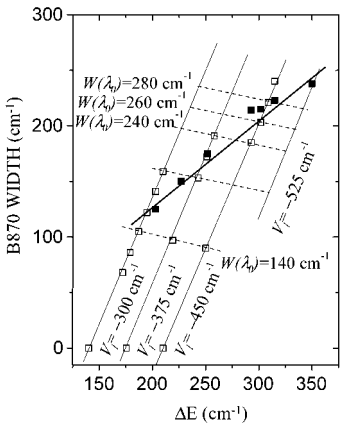

Figure 7. B870 bandwidth vs ΔE and results of numerical simulations with E_{1+} diagonal energy disorder for the case when coupling between upper (u) and lower (l) levels of the B850 ring is neglected. The dark solid line is a liner fit to the experimental $T_p = 190$ K data (solid squares). The thin solid lines are fits to open squares calculated for various fixed values of V_l and varying $W(\lambda_0)$. The calculated dashed lines correspond to different fixed values of $W(\lambda_0)$ and varying V_l. See text for discussion.

Excitonic Calculations with Inclusion of Coupling between the Upper (u) and Lower (l) Exciton Levels That Stem from the Basic Dimer. In the calculations on the effects of pressure on the B850 and B870 bands, dV_u/dp and dV_{ul}/dp were set equal to $-dV_l/dp$ for reasons discussed at the end of section 4 (also see below). Considered first are the values of V_l, $\langle V_{B_1A_2}\rangle$ (eq 7), and $E_u - E_l$ (eqs 2 and 3) at low temperature and ambient pressure. As in the case where coupling between the upper and lower levels was neglected, it was found that a value of -200 cm^{-1} for V_l was too small to account for $\Delta E = 200$ cm^{-1}. On the other hand the value of -320 cm^{-1} from ref 21, which was determined with the neglect of the above coupling is too large. In the preceding subsection, where coupling was also neglected, a value of -315 cm^{-1} was determined. Wu et al.[7,21] concluded that the structure change of LH2 at 150 K increases nearest neighbor couplings of the B850 ring by $\sim$35%. The change is subtle since it has no effect on the B800 band. For this and other reasons they concluded that it is only the $\langle V_{B_1A_2}\rangle$ coupling (eqs 7$-$9) that undergoes a significant increase at 150 K, where B_1 and A_2 are the nearest monomers of adjacent dimers (approximation i). They presented data from pressure experiments which showed that the contribution from the electron-exchange to the coupling between B_1 and A_2 is very important. The same conclusion was reached in ref 8 on the basis of the pressure shift rate of LH2 at room temperature for different bacteria. In the analysis of their pressure data Wu et al.[3] assumed that the coupling between the monomers of the basic dimer $\langle V_{A_1B_1}\rangle = \langle V_{B_1A_2}\rangle$ (approximation ii), so that

$$E_u - E_l = 2\langle V_{B_1A_2}\rangle \qquad (15)$$

On the basis of the analysis of the data in Figure 3 (vide infra) we will arrive at a value of -260 cm^{-1} for V_l. With approximation i, this requires that $\langle V_{B_1A_2}\rangle$ be increased from 290 cm^{-1}

(given in section 4, based on the results of Sauer et al. [19]) to ~420 cm^{-1}. With eq 15, $E_u - E_l$ is increased from 580 to 840 cm^{-1}, which would place all u-exciton levels significantly to the blue of the B800 band (see scheme a of Figure 1 determined using $E_u - E_l = 580$ cm^{-1}).

Considered next are the pressure shift rates for the B850 and B870 bands. With approximation i it follows that the magnitudes of the changes of V_u, V_l, and V_{ul} produced by a change in pressure are the same, δ, which depends on the pressure. Thus, for example, $dV_l/dp = -d\delta/dp$, $\delta > 0$. Also, $dV_l/dp = -2^{-1}\, d\langle V_{B_1A_2}\rangle/dp$ (see eq 7). From the excitonic calculations in which coupling between the upper and lower levels was neglected (preceding subsection) it was found that the contribution from the increase of V_l alone to the shift of the B850 and B870 bands is ~1.5 dV_l/dp and ~2 dV_l/dp, respectively (see Table 3). We remind the reader that these two results were obtained by simulating the dependence of the B870 bandwidth on ΔE, which is hardly affected by coupling between the upper and lower levels. With approximation ii, which leads to eq 15, the equations

$$\text{B850 shift rate} = R_p^m - 2\, d\delta/dp - 1.5\, d\delta/dp \quad (16)$$

and

$$\text{B870 shift rate} = R_p^m - 2\, d\delta/dp - 2\, d\delta/dp + R_p^{ed} \quad (17)$$

should be approximately satisfied, where R_p^m is the monomer shift rate and the second term in the right part stems from eq 15, from which it follows that $dE_l/dp = 2\, dV_l/dp = -2d\delta/dp$. R_p^{ed} is the shift rate due to energy disorder. It is omitted in eq 16 because the results of Table 4 show that energy disorder has a very small effect on the B850 shift rate; see preceding subsection. With the neglect of R_p^{ed} in eq 17 one has from eqs 16 and 17 that

$$\text{B870 shift rate} - \text{B850 shift rate} = -0.5\, d\delta/dp = 0.5\, dV_l/dp \quad (18)$$

From Table 1 the difference in the shift rates is -0.15 cm^{-1}/MPa, so that $d\delta/dp = 0.30$ cm^{-1}/MPa. With this value, eq 16 leads to -1.2 cm^{-1}/MPa for the B850 shift rate (using a monomer shift rate equal to -0.145 cm^{-1}/MPa; vide supra), far too large compared to the experimental value of -0.57 cm^{-1}/MPa. As mentioned, Bchl *a* monomer shift rates fall in the -0.05 to -0.15 cm^{-1}/MPa range and so the discrepancy cannot be explained by the value of the monomer shift rate used. Using the results in Table 4, it was determined that the neglect of R_p^{ed} in eq 17 also does not explain the discrepancy. For the sake of brevity we do not present the details. Given that the two monomers of the basic dimer are energetically inequivalent,[20] we then examined whether that might account for the above discrepancy. On the basis of electronic structure calculations, Alden et al. [20] concluded that the difference in the site excitation energies of the two monomers is ~100 cm^{-1}. Even for a difference of 250 cm^{-1} we found that the correction to the shift rate of the E_l level, $dE_l/dp = -2d\delta/dp$, is no grater than 5%, far too small to account for the discrepancy.

The above findings led us to conclude that the discrepancy is mainly due to eq 15 being invalid; i.e., the coupling between the monomers of the basic dimer is weaker than the coupling between B_1 and A_2 of adjacent dimers. This is consistent with the X-ray structure, which shows that the Mg···Mg distance between B_1 and A_2 and between the monomers of the basic dimer are 8.9 and 9.6 Å, respectively. As a starting point in the simulations of the data in Figure 3 $dE_l/dp \approx dV_l/dp$ (not 2 dV_l/dp) and $E_u - E_l \approx 720$ cm^{-1} (ambient pressure) were taken as initial guesses. As in the preceding subsection it was required that the dependence of the B870 bandwidth on ΔE be accounted for. An iterative procedure was used. The results are shown in Figure 8, and the parameter values obtained are given in Table 5. As expected, the values for dV_l/dp and $dW(\lambda_0)/dp$ of -0.15 and 0.15 cm^{-1}/MPa are similar to those obtained with the neglect of coupling between the u- and l-exciton levels, -0.21 and 0.15 cm^{-1}/MPa. With $E_u - E_l = 720$ cm^{-1}, the coupling between the monomers of the basic dimer is 360 cm^{-1}, compared to the value of 420 cm^{-1} for $\langle V_{B_1A_2}\rangle$, where A_2 and B_1 are the nearest monomers. The latter value was determined using eq 7 with $V_l = -260$ cm^{-1}, $\langle V_{A_1A_2}\rangle = -50$ cm^{-1}, $\langle V_{B_1B_2}\rangle = -36$ cm^{-1}, and $\langle V_{A_1B_2}\rangle = 12$ cm^{-1}. This supports our assertion that $\langle V_{B_1A_2}\rangle$ is larger than the coupling between the monomers of the basic dimer.

The value for $d(E_u - E_l)/dp$ of 0.40 cm^{-1}/MPa was obtained as follows: The calculations showed that the combined contribution from the increase of V_l and $W(\lambda_0)$ to the shift rates of the B850 and B870 bands are -0.225 and -0.375 cm^{-1}/MPa, respectively. The observed shifts are -0.57 and -0.72 cm^{-1}/MPa. The deficit of -0.345 cm^{-1}/MPa is attributable to dE_l/dp and the monomer shift rate. With the latter set to -0.145 cm^{-1}/MPa (vide supra), $dE_l/dp = -0.20$ cm^{-1}/MPa ($\neq 2dV_l/dp$), which means that $d(E_u - E_l)/dp = 0.40$ cm^{-1}/MPa. We emphasize that these parameter values eliminate the inconsistency encountered with eqs 16 and 17 and lead to a value of ~-0.07 cm^{-1}/

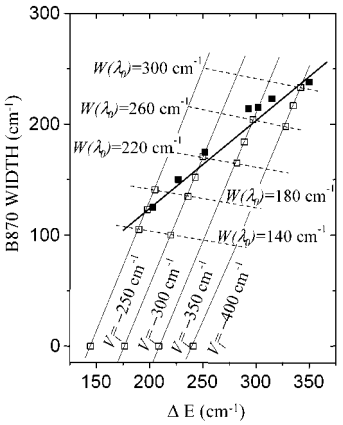

Figure 8. B870 bandwidth vs ΔE and results of numerical simulations with E_{1+} diagonal energy disorder for the case when coupling between upper (u) and lower (l) levels of the B850 ring is included. See Figure 7 caption. Couplings V_u and V_{ul} were varied according to $dV_u/dp = dV_{ul}/dp = -dV_l/dp$; see text.

TABLE 5: Exciton Couplings, Their Pressure Dependencies, and the B800 Shift Rate

parameter	value
V_l (0.1 MPa)	-260 cm^{-1}
V_u (0.1 MPa)	170 cm^{-1}
V_{ul} (0.1 MPa)	195 cm^{-1}
$E_u - E_l$ (0.1 MPa)	720 cm^{-1}
$W(\lambda_0)$ (0.1 MPa)	160 cm^{-1}
dV_l/dp	-0.15 cm^{-1}/MPa
$d(E_u - E_l)/dp$	0.40 cm^{-1}/MPa
dV_u/dp	0.15 cm^{-1}/MPa
dV_{ul}/dp	0.15 cm^{-1}/MPa
$dW(\lambda_0)/dp$	0.15 cm^{-1}/MPa
monomer Bchl *a* energy shift rate	-0.145 cm^{-1}/MPa[a]
B800 band shift rate	-0.115 cm^{-1}/MPa

[a] Determined for the ZPH burned into the B800 band at $\omega_B = 12\,340$ cm^{-1}.

MPa for R_p^{ed}, the contribution of energy disorder alone to the B870's shift rate (indeed smaller than any of the other contributions). With $E_u - E_l = 720$ cm^{-1} it was found that the energy of the monomer of the dimer is 12 300 cm^{-1} (813 nm) at ambient pressure (low-temperature limit). Returning to Figure 8, the ambient pressure point corresponds to $V_l = -260$ cm^{-1} and $W(\lambda_0) = 160$ cm^{-1}, compared to -315 and 160 cm^{-1} from Figure 7. For the 1015 MPa data in Figure 8, $V_l = -410$ cm^{-1} and $W(\lambda_0) = 310$ cm^{-1}, compared to -525 and 310 cm^{-1} from Figure 7. Again, one sees that the inclusion of coupling between the upper and lower levels significantly reduces V_l but has a negligible effect on the width of the distribution function for energy disorder.

According to the calculations that take into account the interaction between upper and lower levels, the integral intensity of B870 band should increase from 9.9% to 10.6% of the total B850 band intensity upon an increase in pressure from 0.1 to 1015 MPa. Such a small increase would not have been observed since the measured value of 5.5% carries an uncertainty of $\pm$1.5%. The apparent discrepancy of a factor of 2 between the calculated and observed percentages is reduced by taking into account the low-energy ($\sim$150$-$400 cm^{-1}) Bchl *a* vibrations that build on the B870 band and contribute to the B850 band. Based on the Franck$-$Condon factors in ref 49, the reduction is about 1.5%. Thus, the agreement between theory and experiment is quite reasonable.

To conclude this section, we compare some of our findings with those of Jang et al.,[24] who, guided by the results from the first-order degenerate perturbation theory, performed detailed simulations on the effects of energy disorder on the B850 and B870 bands at ambient pressure and liquid helium temperatures. Independent Gaussian diagonal and off-diagonal energy disorder, as well as negatively and positively correlated combinations of the two, were considered. Linear interdependencies (common scaling law) for ΔE (gap between the E_{1l} level and the B870 level), the B870 bandwidth, the bandwidths of the two E_{1l} components and the splitting of the E_{1l} level were found to hold. The results in Figures 3 and 8 are entirely consistent with that prediction and, moreover, further justify our use of the E_{1+} BDP for diagonal disorder. That is, the effects of Gaussian random disorder on the B850 and B870 bands are similar to the effects of E_{1+} disorder. Our results establish that the pressure dependences of energy disorder and nearest neighbor couplings are positively correlated. This was not considered by Jang et al.[24] Further testing of the theory in their paper would require hole burning and single complex spectroscopic studies with samples of different quality at ambient pressure, i.e., degree of the inhomogeneous broadening of the B850 and B870 bands. It is not apparent that the results of such experiments would establish the positive correlation between energy disorder and nearest neighbor couplings revealed here. Clearly, the use of pressure with the above two spectroscopies would be the preferred approach for studying the interplay between energy disorder and excitonic couplings.

B. Additional Decay Channel of the B800 Band. The ZPH width results for the B800 band at ambient pressure and 875 MPa in Figure 5, as well as the data for 290, 610, and 1015 MPa (not shown), reveal that the onset for the increase of the ZPH width tracks the shift of the B800 band with pressure. For all pressures the onset is 27 $\pm$ 5 cm^{-1} to the blue of the B800 band maximum. This suggests that mixed B800$-$B850 states involving the upper levels of the B850 ring (in the near vicinity of the B800 band) may not be important for the additional decay channel; see Introduction. The positions of those upper levels in scheme b of Figure 1 were calculated using the values of V_l, V_u, V_{ul}, and $E_u - E_l$ given in Table 5. Except for the E_{4u} level, they lie on the high-energy side of the B800 band and, as suggested in ref 5, may be responsible for the tailing of the B800 band on its high-energy side. This would require mixing of the upper levels with B800 levels. Since B800$-$B850 couplings as strong as $\sim$30 cm^{-1} exist,[19] such mixing must occur, it is just a question of its extent. In this regard, we note that there should be no symmetry restrictions since the B800 excitations are highly localized due to energy disorder. A first step in understanding how pressure affects the coupling between the B800 levels and B850 levels in their proximity is to calculate the shift rates of the latter in the absence of disorder, keeping in mind that the shift rate for the B800 levels is -0.145 cm^{-1}/MPa. The results for the A_u, E_{1u}, E_{4l}, E_{2u}, and E_{3u} levels are given in Table 6. They were obtained with the values of dV_l/dp, dV_u/dp, dV_{ul}/dp, $d(E_u - E_l)/dp$, and the monomer shift rate given in Table 5. The shift rates are all positive. For the four upper levels this is the result of $dE_u/dp = 0.2$ cm^{-1}/MPa being greater in magnitude than the monomer shift rate of -0.145 cm^{-1}/MPa and the pressure-induced changes of coupling energies V_l and V_u tending to shift the upper levels of the B850 ring to higher and lower energies, respectively. The next question is how energy disorder affects the shift rates in Table 6. Preliminary calculations showed that the shift rates for higher and lower upper levels under consideration increase and decrease, respectively, as might be expected on the basis of perturbation theory. However, the changes in shift rates are small and only the E_{3u} level exhibited a (small) negative shift rate. In view of this and the results in Figure 6 and Table 6, we conclude that mixing of B800 and upper B850 levels is too weak to account for the additional decay channel, contrary to what was proposed by Wu et al.[5]

TABLE 6: Pressure Shift Rates of the B850 Levels in the Vicinity of the B800 Band

level	press. shift rate (cm^{-1}/MPa)
A_u	0.437
E_{1u}	0.341
E_{4l}	0.146
E_{2u}	0.112
E_{3u}	0.008

The proposition of Wu et al. was based on a simple Förster-type model for B800 $\rightarrow$ B800 downward energy transfer that proved to be inconsistent with ambient pressure data of the type shown in Figure 6. The model took into account the B800 site distribution function and spectral density for downward transfer. The mixed B800$-$B850 state mechanism then won out by default. That is, data of the type shown in Figure 6 for higher pressures were not available to Wu et al. However, not taken into account in their model is that the energy transfer rate from an initially excited B800 molecule with a nearest neighbor having lower excitation energy is much higher than when this is not the case. Based on the structure of the LH 2 and the R^{-6} dependence of the Förster transfer rate, the rate between nearest neighbors should be about 40 times higher than between next-nearest neighbors.

With this in mind, we present a simple combinatorial model that restricts downward B800 $\rightarrow$ B800 transfer from a given Bchl *a* molecule to a nearest neighbor whose excitation energy is lower. The reasonable assumptions that there is no correlation between the position of a molecule in a C_9 ring and its absorption frequency and that there are no accidental degeneracies are made. The sites are denoted by L_n, $n = 1, ..., 9$, where $n = 1$ for the lowest energy site in any given ring. Obviously,

and independent of any model, one-ninth of the sites in an ensemble (L_1 sites) are incapable of downward energy transfer in the B800 manifold since there are no B800 molecules in the ring absorbing lower in energy. Concerning L_2, the probability that L_1 is its nearest neighbor is 2/8, thus the probability of L_2 sites being incapable of downward energy transfer is 3/4. It is not difficult to show that the probability of site L_n being incapable of downward transfer is (for $n = 1, ..., 7$) given by $9 \cdot 2 \cdot 6! \cdot C_{2,9-n}/9!$, where $C_{2,9-n} = (9 - n)!/2!(9 - n - 2)!$. Thus, for example, this probability is 1/28 for $n = 7$ (third highest energy). Note that the probability for $n = 8$ and 9 is zero. Totally, one-third of all B800 Bchl *a* molecules will be capable only to the B800 → B850 energy transfer, but not to the B800 → B800 energy transfer. The majority of these molecules will absorb to the red of the B800 maximum. The distribution of molecules incapable of B800 → B800 energy transfer is visualized by the ZPH action spectrum normalized to account for approximately one-third of the total B800 absorption (dotted curve in Figure 6). Since the dashed and dotted curves in Figure 6 overlap, the question arises as to whether it is consistent with the hole width being constant at lower energies (Figure 5). There is no inconsistency, since the measured holes were shallow and the hole burning efficiency of the sites associated with the additional decay channel is about a factor of 8 lower than for sites that are not. Thus, the broader contribution to the hole profiles from the former sites would be unobservable. The observations (see Results and Table 2) that the fraction of B800 molecules incapable of intraband energy transfer (1/3) as well as the ratios between parameters of the action spectra and of the B800 band remain the same at higher pressures agree with our model and further support the assertion that the mixing of B800 and B850 states is of little importance.

The model presented here explains the hole width data in Figure 5 qualitatively. Detailed calculations of the Q_y electronic structure and intraband energy transfer rates of the B800 ring that take into account the next-nearest neighbor interactions and energy disorder, together with data from further single complex spectroscopic studies, are required to determine if the B800 → B800 intraband transfer mechanism can quantitatively account for the results in Figure 5. With that remark we discuss some possible consequences of our model. For example, it can explain qualitatively why a B800 → B800 energy transfer rate of 400 fs was observed for an excitation wavelength of 783 nm.[5] The absorption in that region, at significantly higher energy than the B800 band maximum, is dominated by L_8 and L_9 states, both of which have both nearest neighbors absorbing at lower energy. The distribution of molecules that have both nearest neighbors absorbing at lower energy is a mirror image of the distribution of molecules incapable of energy transfer; i.e., for the second highest energy molecule (L_8), the probability that both neighbors absorb at lower energy is 3/4 and so on (vide supra). The L_8 and L_9 molecules should have a 2 times higher rate of downward energy transfer than molecules having only one lower energy nearest neighbor. If for the latter fraction the B800 → B800 transfer rate is ~1 ps, for the former fraction it should be close to 500 fs, in reasonable agreement with values in ref 5.

Finally, it should be noted that the above model does not account for the dependence of the transfer rate on the energy gap between the donor and acceptor sites. In this regard, the results of calculations[5] that employed a reasonable value for nearest neighbor coupling energy and took into account electron−phonon coupling showed that ~1 ps transfer time is possible when the donor−acceptor energy gap is close to the observed peak phonon energy of ~30 cm^{-1}. Femtosecond experiments led to an estimate of 0.5 ps for the transfer time.[5,50,51]

6. Concluding Remarks

The experimental results presented establish, for the first time, that the pressure dependences of observables of great importance for understanding the excitonic structure of the B850 ring of LH 2 are linearly correlated. They are the positions and widths of the B850 and B870 bands (Figure 3). Excitonic calculations were performed in the nearest dimer−dimer coupling approximation with diagonal energy disorder. By fitting the linear pressure shift rates of the B850 and B870 bands and the broadening of the B870 band (using an experimental value for the monomer energy shift rate), an effective pressure-dependent Hamiltonian for the B850 ring was obtained. The pressure dependences of the coupling terms (in eqs 2−4), V_l, V_u, V_{ul}, and $E_u - E_l$, along with their ambient pressure (5 K) values are given in Table 5.

At ambient pressure the monomer excitation energy associated with the basic dimer, with splitting $E_u - E_l$, is predicted to be 12 300 cm^{-1} (813 nm). An assumption of the model is that the pressure shift rates of V_l, V_u, and V_{ul} are mainly dictated by the coupling between the nearest monomers of adjacent dimers ($\langle V_{B_1A_2} \rangle$ in eqs 7−9). Based on the results in ref 3, which show that electron-exchange coupling between nearest neighbors makes the largest contribution to the pressure shift rates of the B850 exciton levels, the above assumption seems reasonable. It leads to the magnitudes of dV_u/dp, dV_l/dp, and dV_{ul}/dp being equal, Table 5. An important finding is that the magnitudes of nearest neighbor coupling energies and the half-width ($W(\lambda_0)$) of the energy disorder distribution are linearly correlated, with both increasing with pressure; see, e.g., Figure 8. The presence of some positive correlation is expected if there is no pressure-induced ordering in LH 2 complexes. Increase of pressure results in the decrease of distances between chlorophyll molecules and alterations of interactions between chlorophylls and other surrounding molecules. Both electrostatic and electron-exchange couplings increase with a decrease of inter-chlorophyll distances (R). As long as the fractional change $\Delta R/R$ is small enough, both couplings grow linearly with pressure[3]. For $\Delta p = 1000$ MPa and a typical compressibility (κ) of 0.1 GPa^{-1}, $\Delta R/R = 0.03$, in reasonable agreement with V_l increasing from 260 to 410 cm^{-1}, with the increase due mainly to electron-exchange coupling. The increase of inhomogeneous bandwidth with pressure has been theoretically treated by Laird and Skinner[52] and observed in a variety of systems, for example, polymers.[53] In the simplest case when the interactions between chromophore and surrounding molecules are dispersive ($\sim R^{-6}$), the pressure-induced shift of a chromophore's absorption frequency is proportional to pressure and to the absorption frequency of that molecule at ambient pressure: $d\nu/dp = 2\kappa(\nu - \nu_{vac})$.[46] Here ν_{vac} is the absorption frequency of the chromophore molecule in the gas phase. In other words, the larger the solvent shift, the larger is the pressure-induced shift. Of course, in the case of chlorophyll in protein environment the assumptions leading to such a simple equation are not quite satisfied (positions of molecules are in fact correlated, not only dispersive interactions are present and the complex is neither homogeneous nor isotropic). Nevertheless, the behavior of the inhomogeneous band is qualitatively similar (see ref 46 for reasoning); i.e., inhomogeneous broadening should increase with pressure. Consequently, the half-width $W(\lambda_0)$ should increase with pressure since in the case of diagonal energy disorder it is simply

proportional to inhomogeneous bandwidth. It would be interesting to carry out molecular dynamics and electronic structure calculations on LH 2 under pressure, such as those performed on LH 2 of *Rs. molischianum* at ambient pressure.[30] Of particular interest would be an assessment of the relative contributions of electron-exchange and electrostatics to nearest neighbor coupling energies in the B850 ring. The results might also provide additional insight on why the pressure dependences of nearest neighbor couplings and energy disorder are linearly correlated.

Concerning the ambient pressure exciton level scheme b in Figure 1 (low-temperature limit), we consider it to be reliable. It correctly predicts the positions of the A_l (B870) and E_{2l} levels. The E_{3u}, E_{2u}, E_{4l}, E_{1u}, and A_u levels are all located on the high-energy side of the B800 band. Due to coupling (weak) with B800 levels, they are probably responsible for the high-energy tailing of the B800 band. The low-energy side of the B800 band has a Gaussian shape (characteristic of inhomogeneous broadening), consistent with no upper (u) levels lying in that energy region.

Only Gaussian diagonal energy disorder was considered and only of the E_1 symmetry since it governs the response of the B870 level to disorder. We emphasize again that our simulations on the effects of pressure on excitonic structure focused on the width of the B870 band and its displacement (ΔE) from the B850 band, Figures 7 and 8. Because the weak energy disorder limit applies, E_1 off-diagonal disorder should lead to similar results. As discussed in refs 24, 31, and 32, both types of disorder are likely to be present. To determine the effects of disorder on the overall exciton level structure seen in scheme b of Figure 1 would require Monte Carlo simulations with random energy disorder (diagonal and off-diagonal) of the type in ref 24 using our ambient pressure, low-temperature Hamiltonian defined in Table 5.

The experimental data used to obtain the results in Table 5 are for a pressurization temperature (T_p) of 190 K. We fully expect that the above linear interdependencies and correlations will exist for lower T_p values since pressure-induced structural changes are elastic, at least for the pressures used here. At higher T_p values and pressures plastic behavior can occur, as we have shown for $T_p = 230$ K, and prevent straightforward analysis of the data. Using the results in Table 1, we estimate that for $T_p =$ 80 K, $dV_u/dp = dV_{ul}/dp = -dV_l/dp = 0.11$ cm^{-1}/MPa, $dW(\lambda_0)/dp = 0.11$ cm^{-1}/MPa, and $d(E_u - E_l)/dp = 0.20$ cm^{-1}/MPa, significantly smaller than the values in Table 5 due to reduced compressibility at 80 K. At this time we are not able to estimate values of the above pressure shift rates at room temperature, but they should be somewhat larger than the $T_p = 190$ K values.

The last part of the paper dealt with the additional decay channel of the B800 band. The high-pressure hole burning data indicate that the additional channel is not due to mixed B800−B850 states involving upper levels of the B850 ring. A simple combinatorial model was presented that qualitatively explains the hole width results in Figure 5. It restricts downward energy transfer to nearest neighbors in the B800 ring. It predicts that the only decay channel for one-third of the B800 sites is B800 → B850 transfer while the remaining and higher energy absorbing sites can, in addition, undergo intra-B800 band transfer, as illustrated in Figure 6. Calculations in which experimentally determined spectral density due to phonons and energy disorder are taken into account would further test the model.

Acknowledgment. Research at the Ames Laboratory was supported by the Division of Chemical Sciences, Office of Basic Energy Sciences, U.S. Department of Energy. Ames Laboratory is operated for USDOE by Iowa State University under Contract W-7405-Eng-82. We thank Satoshi Matsuzaki for assistance in setting up high-pressure experiments, Professor R. Cogdell, University of Glasgow, for providing the LH 2 samples and Professor R. J. Silbey, MIT, for providing refs 24 and 34 prior to their publication. We are indebted to Dr. John M. Hayes for reading this paper and for valuable suggestions.

References and Notes

(1) Pieper, J.; Rätsep, M.; Jankowiak, R.; Irrgang, K.-D.; Voigt, J.; Renger, G.; Small, G. J. *J. Phys. Chem. A* **1999**, *103*, 2412.
(2) Chang, H.-C.; Jankowiak, R.; Reddy, N. R. S.; Small, G. *J. Chem. Phys.* **1995**, *197*, 307.
(3) Wu, H.-M.; Rätsep, M.; Jankowiak, R.; Cogdell, R. J.; Small, G. J. *J. Phys. Chem. B* **1998**, *102*, 4023.
(4) Sturgis, J. N.; Gall, A.; Ellervee, A.; Freiberg, A.; Robert, B. *Biochemistry* **1998**, *37*, 14875.
(5) Wu, H.-M.; Savikhin, S.; Reddy, N. R. S.; Jankowiak, R.; Cogdell, R. J.; Struve, W. S.; Small, G. J. *J. Phys. Chem.* **1996**, *100*, 12022.
(6) Reddy, N. R. S.; Wu, H.-M.; Jankowiak, R.; Picorel, R.; Cogdell, R. J.; Small, G. *J. Photosynth. Res.* **1996**, *48*, 277.
(7) Wu, H.-M.; Rätsep, M.; Jankowiak, R.; Cogdell, R. J.; Small, G. J. *J. Phys. Chem. B* **1997**, *101*, 7641.
(8) Timpmann, K.; Ellervee, A.; Pullerits, T.; Ruus, R.; Sundström, V.; Freiberg, A. *J. Phys. Chem. B* **2001**, *105*, 8436.
(9) Rätsep, M.; Johnson, T. W.; Chitnis, P. R.; Small, G. J. *J. Phys. Chem. B* **2000**, *104*, 836.
(10) Zazubovich, V.; Matsuzaki, S.; Johnson, T. W.; Hayes, J. M.; Chitnis, P. R.; Small, G. *J. Chem. Phys.* **2002**, *275*, 47.
(11) Wu, H.-M.; Rätsep, M.; Young, C. S.; Jankowiak, R.; Small, G. J. *Biophys. J.* **2000**, *79*, 1.
(12) Reddy, N. R. S.; Jankowiak, R.; Small, G. J. *J. Phys. Chem.* **1995**, *99*, 16168.
(13) Rätsep, M.; Wu, H.-M.; Hayes, J. M.; Blankenship, R. E.; Cogdell, R. J.; Small, G. J. *J. Phys. Chem. B* **1998**, *102*, 4035.
(14) van Grondelle, R.; Dekku, J. P.; Gillbro, T.; Sundström, V. *Biochim. Biophys. Acta* **1994**, *1187*, 1; Pullerits, T.; Sundström, V. *Acc. Chem. Res.* **1996**, *29*, 381.
(15) Sundström, V.; van Grondelle, R. In *Anoxygenic Photosynthetic Bacteria*; Blankenship, R. E., Madigan, M. T., Baller, C. E., Eds.; Kluwer Academic Publishers: Dordrecht, The Netherlands, 1995; p 349.
(16) Freer, A. A.; Prince, S. M.; Sauer, K.; Papiz, M. Z.; Hawthornewaite-Lawless, A. M.; McDermott, G.; Cogdell, R. J.; Isaacs, N. W. *Structure* **1996**, *4*, 449.
(17) Koepke, J.; Xu, X.; Muenke, C.; Schulten, K.; Michl, H. *Structure* **1996**, *4*, 561.
(18) Sundström, V.; Pullerits, T.; van Grondelle, R. *J. Phys. Chem. B* **1999**, *103*, 2327.
(19) Sauer, K.; Cogdell, R. J.; Prince, S. M.; Freer, A. A.; Isaacs, N. W.; Scheer, H. *Photochem. Photobiol.* **1996**, *64*, 564.
(20) Alden, R. G.; Johnson, E.; Nagarajan, V.; Parson, W. W.; Law, C.; Cogdell, R. J. *J. Phys. Chem. B* **1997**, *101*, 4667.
(21) Wu, H.-M.; Rätsep, M.; Lee, I.-J.; Cogdell, R. J.; Small, G. J. *J. Phys. Chem. B* **1997**, *101*, 7654.
(22) Linnanto, J.; Korppi-Tommola, J. I. I.; Helenius, V. M. *J. Phys. Chem. B* **1999**, *103*, 8739.
(23) Mukai, K.; Abe, S.; Sumi, H. *J. Phys. Chem. B* **1999**, *103*, 6096.
(24) Jang, S.; Dempster, S. E.; Silbey, R. J. *J. Phys. Chem. B* **2001**, *105*, 6655.
(25) Krueger, B. P.; Scholes, G. D.; Fleming, G. R. *J. Phys. Chem. B* **1998**, *102*, 5378.
(26) Scholes, G. D.; Gould, I. R.; Cogdell, R. J.; Fleming, G. R. *J. Phys. Chem. B* **1999**, *103*, 2543.
(27) Hu, X.; Ritz, T.; Damjanovic, A.; Schulten, K. *J. Phys. Chem. B* **1997**, *101*, 3854.
(28) Cory, M. G.; Zerner, M. C.; Hu, X.; Schulten, K. *J. Phys. Chem. B* **1998**, *102*, 7640.
(29) Dahlbom, M.; Pullerits, T.; Mukamel, S.; Sundström, V. *J. Phys. Chem. B* **2001**, *105*, 5515.
(30) Damjanovic, A.; Kozstin, I.; Kleinekathoefer, U.; Shulten, K. *Phys. Rev. E* **2002**, *65*, 031919.
(31) Wu, H.-M.; Small, G. J. *J. Phys. Chem. B* **1998**, *102*, 888.
(32) Wu, H.-M.; Small, G. J. *Chem. Phys.* **1997**, *218*, 225.
(33) Wu, H.-M.; Reddy, N. R. S.; R. J.; Small, G. J. *J. Phys. Chem. B* **1997**, *101*, 651.
(34) Dempster, S. E.; Jang, S.; Silbey, R. J. *J. Chem. Phys.* **2001**, *114*, 10015.

(35) Matsushita, M.; Ketelaars, M.; van Oijen, A. M.; Köhler, J.; Aartsma, T. J.; Schmidt, J. *Biophys. J.* **2001**, *80*, 1591.
(36) Ketelaars, M.; van Oijen, A. M.; Matsushita, M.; Köhler, J.; Aartsma, T. J. Schmidt, J. *Biophys. J.* **2001**, *80*, 1604.
(37) De Caro, C.; Visschers, R. W.; van Grondelle, R.; Völker, S. *J. Phys. Chem.* **1994**, *98*, 10584.
(38) van Oijen, A. M.; Ketelaars, M.; Köhler, J.; Aartsma, T. J.; Schmidt, J. *Biophys. J.* **2000**, *78*, 1570.
(39) Koolhaas, M. H. C.; Frese, R. N.; Fowler, G. J. S.; Bibby, T. S.; Georgakopoulu, S.; van der Zwan, G.; Hunter, C. N.; van Grondelle, R. *Biochemistry* **1998**, *37*, 4693.
(40) Matsuzaki, S.; Zazubovich, V.; Fraser, N. J.; Cogdell, R. J.; Small, G. J. *J. Phys. Chem. B* **2001**, *105*, 7049.
(41) Reddy, N. R. S.; Picorel, R.; Small, G. J. *J. Phys. Chem.* **1992**, *96*, 6458.
(42) Zollfrank, J.; Friedrich, J.; Fidy, J.; Vanderkooi, J. M. *J. Chem. Phys.* **1991**, *94*, 8600.
(43) Zollfrank, J.; Friedrich, J.; Parak, F. *Biophys. J.* **1992**, *61*, 716.
(44) Balog, E.; Kis-Petik, K.; Fidy, J.; Köhler, M.; Friedrich, J. *Biophys. J.* **1997**, *73*, 397.
(45) Fidy, J.; Vanderkooi, J. M.; Zollfrank, J.; Friedrich, J. *Biophys. J.* **1992**, *63*, 1605.
(46) Köhler, M.; Friedrich, J.; Fidy, J. *Biochim. Biophys. Acta* **1998**, *1386*, 255.
(47) Smeller, L.; Fidy, J. *Biophys. J.* **2002**, *82*, 426.
(48) Fidder, H.; Knoester, J.; Wiersma, D. A. *J. Chem. Phys.* **1991**, *95*, 7880.
(49) Zazubovich, V.; Tibe, I.; Small, G. J. *J. Phys. Chem. B* **2001**, *105*, 12410.
(50) Monshouwer, R.; de Zarate, I. O.; van Mourik, F.; van Grondelle, R. *Chem. Phys. Lett.* **1995**, *246*, 341.
(51) Monshouwer, R.; van Grondelle, R. *Biochim. Biophys. Acta*. **1996**, *1275*, 70.
(52) Laird, B. B.; Skinner, J. L. *J. Chem. Phys.* **1989**, *90*, 3274.
(53) Clark, F. T.; Drickamer, H. G. *J. Phys. Chem.* **1986**, *90*, 589.